

The effect of Congo River freshwater discharge on Eastern Equatorial Atlantic climate variability

Stefano Materia · Silvio Gualdi · Antonio Navarra · Laurent Terray

Received: 14 April 2011 / Accepted: 27 August 2012 / Published online: 18 September 2012
© Springer-Verlag 2012

Abstract The surface ocean explains a considerable part of the inter-annual Tropical Atlantic variability. The present work makes use of observational datasets to investigate the effect of freshwater flow on sea surface salinity (SSS) and temperature (SST) in the Gulf of Guinea. In particular, the Congo River discharges a huge amount of freshwater into the ocean, affecting SSS in the Eastern Equatorial Atlantic (EEA) and stratifying the surface layers. The hypothesis is that an excess of river runoff emphasize stratification, influencing the ocean temperature. In fact, our findings show that SSTs in the Gulf of Guinea are warmer in summers following an anomalously high Congo spring discharge. Vice versa, when the river discharges low freshwater, a cold anomaly appears in the Gulf. The response of SST is not linear: temperature anomalies are considerable and long-lasting in the event of large freshwater flow, while in dry years they are less remarkable, although still significant. An excess of freshwater seems able to form a barrier layer, which inhibits vertical mixing and the entrainment of the cold thermocline water into the surface. Other processes may contribute to SST variability, among which the net input of atmospheric freshwater falling over EEA. Likewise the case of continental runoff from Congo River, warm anomalies occur after

anomalously rainy seasons and low temperatures follow dry seasons, confirming the effect of freshwater on SST. However, the two sources of freshwater anomaly are not in phase, so that it is possible to split between atypical SST following continental freshwater anomalies and rainfall anomalies. Also, variations in air-sea fluxes can produce heating and cooling of the Gulf of Guinea. Nevertheless, atypical SSTs cannot be ascribed to fluxes, since the temperature variation induced by them is not sufficient to explain the SST anomalies appearing in the Gulf after anomalous peak discharges. The interaction processes between river runoff, sea surface salinity and temperature play an effective role in the interannual variability in the EEA region. Our results add a new source of variability in the area, which was often neglected by previous studies.

1 Introduction

Several reasons make the tropical Atlantic variability a challenging issue for the scientific community. First, many coupled general circulation models (AOGCMs) show severe biases in the representation of Tropical Atlantic main features. For instance, models fail to capture the cold tongue in Eastern Equatorial Atlantic (EEA), inducing a reversal of the climatological SST gradient (Davey et al. 2002; Richter and Xie 2008), which is determinant in a region where surface ocean explains a considerable fraction of the total variability (Mehta 1998). Besides, spring precipitation is generally overestimated south of the equator, leading to the presence of a double Inter-Tropical Convergence Zone (ITCZ; Breugem et al. 2007; Stockdale et al. 2006).

On the other hand, a good understanding of tropical Atlantic is fundamental since its impacts affect a large rural

S. Materia (✉) · S. Gualdi · A. Navarra
Centro Euro-Mediterraneo per i Cambiamenti Climatici,
Bologna, Italy
e-mail: stefano.materia@cmcc.it

S. Gualdi · A. Navarra
Istituto Nazionale di Geofisica e Vulcanologia, Bologna, Italy

L. Terray
Sciences de l'Univers au CERFACS, URA1875 CERFACS/
CNRS, Toulouse, France

population, which sources of sustenance are strongly dependent on precipitation (Polo et al. 2008). Furthermore, many studies have focused on the link between tropical Atlantic variability and mid-latitude climate at seasonal (Van den Dool et al. 2006) and decadal (Mehta and Delworth 1995) time scales.

The aim of this study is to improve our understanding of climate variability in the Tropical Atlantic, accounting for the forcing represented by the continental freshwater discharge (FWD), neglected in the majority of previous studies. Our prime objective is to understand the interactions between freshwater discharge and ocean circulation in EEA. In this region a huge quantity of freshwater is collected due to heavy rainfall and discharge from several rivers. The Congo River alone, whose drainage basin covers 4 million km² over Central Africa (Fig. 1), releases every year 1,270 km³ of freshwater into the ocean (Weldad et al. 2007), which is the second-largest flow in the world second only to the Amazon River. Niger, Sanaga, Volta and other smaller catchments contribute to further

increase the amount of freshwater draining into the Gulf of Guinea.

The understanding of feedbacks in this area is crucial because SSTs in the Gulf of Guinea demonstrated to affect precipitation over part of western Africa. The rainfall patterns in the region are related to the mean meridional circulation, described by a near surface monsoon flow that transfers water evaporated over the Gulf of Guinea to the African continent (Hourdin et al. 2010). As a consequence, SST anomalies (SSTAs) in the Gulf would play an important role in driving precipitation patterns, specifically in the region overlooking the Gulf. According to Giannini et al. (2005), the Guinea coast rainfall depends on Atlantic Ocean variability, and particularly on the EEA SSTs. The Sahel pattern, instead, represents variability of the African monsoon and displays a remarkable amount of noise. Correlations between Gulf of Guinea SSTs and precipitation in Sahel were negative until the early 70's, and not significant in the last 30 years (Joly and Voltaire 2009).



Fig. 1 Course and watershed of the Congo River with topography shading. Courtesy of Imagico (www.imagico.de), under Creative Common Attribution-Share Alike 2.5 Generic License (<http://creativecommons.org/licenses/by-sa/2.5/deed.en>). The CEA index is also drawn

The main mode of interannual variability in the Gulf is the so-called “Atlantic Niño” (e.g. Covey and Hastenrath 1978; Philander and Pacanowski 1986; Zebiak 1993) an internal equatorial Atlantic oscillation that involves coupled processes similar to those generating ENSO (Latif and Grötzner 2000), but with different time-scales. It is characterized by the mitigation of the cold tongue in the EEA during late spring and early summer.

Congo River discharge anomaly may contribute to this variability. In the early nineties, a few studies pointed out the impact of FWD on the ocean circulation (Lukas and Lindstrom 1992; Sprintall and Tomczak 1992) through a mechanism known as the barrier layer. Due to low saline water entering the ocean from precipitation or river discharge, an isothermal layer with strong salinity stratification forms between the top of the thermocline and the bottom of the mixed layer. It is called barrier layer because it reduces the entrainment and vertical turbulent mixing of cold thermocline water into the upper layers (Vinayachandran and Nanjundiah 2009).

The effect of continental FWD on the SST has not been extensively examined in this area so far. Carton (1991) evaluated the diverse sources of freshwater in the whole Tropical Atlantic making use of an ocean model. He concluded that the absence of freshwater flux would lead to instability of the upwelling region driven by the increase of salinity. This would intensify vertical mixing and allow increased entrainment of the thermocline cold water, which cools the mixed layer and, to a lesser extent, the SST. In particular, the inclusion of freshwater causes the strongest SSTA off the Congo mouth, beginning near the coast, and then moving offshore. Dessier and Donguy (1994) state that SSS variability in Western Tropical Atlantic is largely related to river outflow, while in Eastern Tropical Atlantic (ETA) precipitation associated with the ITCZ has a major control on the SSS seasonality. The Gulf of Guinea region, however, is an exception because of the presence of the Congo River discharge.

The role of FWD on oceanic features has been more deeply investigated in other regions. Several works have been carried out on the Western Tropical Atlantic, where Amazon and Orinoco Rivers spread into the ocean. Field (2007) states that the two freshwater flows combine to form an extensive buoyant plume, whose temperature is so elevated that hurricanes passing over that region are influenced by ocean–atmosphere interaction with the plume prior to reaching the Caribbean. Hellweger and Gordon (2002) found high correlation between Barbados sea surface salinity (SSS) and Amazon discharge lagged by two months (the travel time from Amazon mouth and the Caribbean).

Park et al. (2011) conclude that Chang Jiang river discharge contributes to SST increase in the East China Sea in August. The warming is caused by the formation of a barrier

layer that enhances stratification by reducing vertical mixing and entrainment. Using an ocean model, Chamathi and Ram (2009) state that freshwater inflow is a strong forcing that drives the Bay of Bengal circulation. Coastal upwelling is suppressed by the continental freshwater discharge, and consequently an experiment in which FWD is suppressed shows very low SSTs appearing off the shoreline. Besides, along the coast, surface currents lose their equator-ward component in favour of a north-westward direction. Chamathi et al. (2008) point out that river runoff forms a highly stratified layer, which has the effect of reducing the mixed layer depth along the coast. Vertical mixing is inhibited even during summer, despite the strong monsoon winds. Again, the coastal upwelling is suppressed by the presence of FWD. These findings are consistent with Vinayachandran et al. (2002), who observed a rapid thinning of the mixed layer after a heavy rain event on the ocean during monsoon season.

Owing to the periodic movement of the ITCZ across the equator (Fig. 2b), the Congo River shows two peak discharges in December and May (Fig. 2a). Although the first one is the largest peak discharge, our study focuses on the secondary maximum because the freshwater drained into the Atlantic moves towards the Gulf of Guinea during the early summer, that is the season characterized by the maximum SST variance (Joly and Voldoire 2009). Therefore, the effect of the secondary peak can play a role in the onset of the West African Monsoon, which is found to be sensitive to the interannual variability of SST in the region (Gu and Adler 2004). Besides, observations show that, on average, no barrier layer characterizes the ETA region in boreal summer, but excessive freshwater input, like the ones simulated by many GCMs, can be crucial in developing it (Breugem et al. 2008).

In this work we examine how the variability associated with continental freshwater discharge may be involved in the mechanisms that regulate the climate of EEA. In particular, we investigate the effect of the Congo River secondary peak discharge on SSS and SST in Gulf of Guinea, analyzing observational data covering 50 years. The methodology applied and the data used are illustrated in Sect. 2, while in Sect. 3 we describe the seasonal cycle of SST in the Gulf, rainfall in the river drainage basin and Congo discharge, and we perform a brief analysis on rainfall anomalies in the Congo watershed. The effect of freshwater discharge and other causes of SST variability in the ocean is examined in Sects. 4, and 5 finally contains a discussion of new outcomes and some preliminary conclusion.

2 Data and methodology

This study makes use of several observational gridded datasets, provided on a monthly basis, to characterize the climate of the region and its variability.

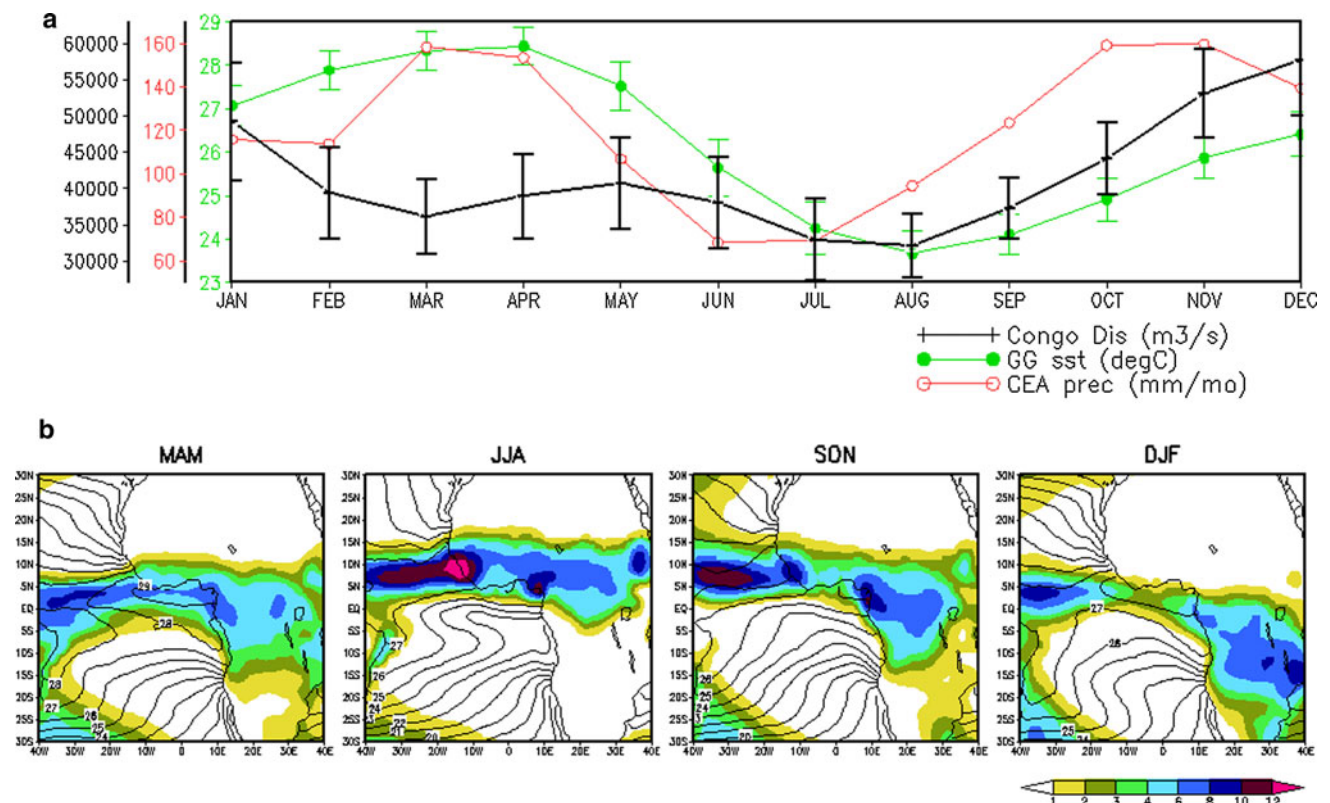


Fig. 2 **a** Mean annual cycle of precipitation (CRU dataset) over Central Equatorial Africa, SST in the Gulf of Guinea and discharge of Congo River at Brazzaville. **b** Seasonal cycle of SST in EEA and precipitation (GPCP dataset) in ETA and Africa

Congo River discharge data have been supplied by the Global Runoff Data Centre (GRDC 2011) for Brazzaville station (15.31°E, 4.26°S), about 400 km upstream the river mouth. On land, CRU TS 2.1 (Mitchell and Jones 2005) was used for a preliminary examination on precipitation over Central Equatorial Africa (CEA), which mostly covers the Congo watershed (see also Todd and Washington 2004), at 0.5° regular horizontal grids.

In the ocean, we used the EN3 quality controlled subsurface ocean salinity data, at a global 1° regular horizontal grid (Ingleby and Huddleston 2007) provided by the Hadley Center. The Hadley Center HadSST2 improved database (Rayner et al. 2006) at 1° regular horizontal grid was the SST reference. The Global Precipitation Climatology Project (GPCP version 2.1, Adler et al. 2003), observational rainfall at 2.5° resolution from 1979, and the Objectively Analyzed air-sea Heat Fluxes (OAFlux, Yu et al. 2008), ocean evaporation data at 1° resolution, were used to analyze atmospheric freshwater fluxes in the Gulf of Guinea.

We made use of the ERA40 2.5° reanalysis (Uppala et al. 2007) to evaluate surface winds, heat fluxes and surface net radiation in the Gulf of Guinea, and the 2° resolution global climatology, based on individual temperature and salinity profiles, of the mixed layer depth (de

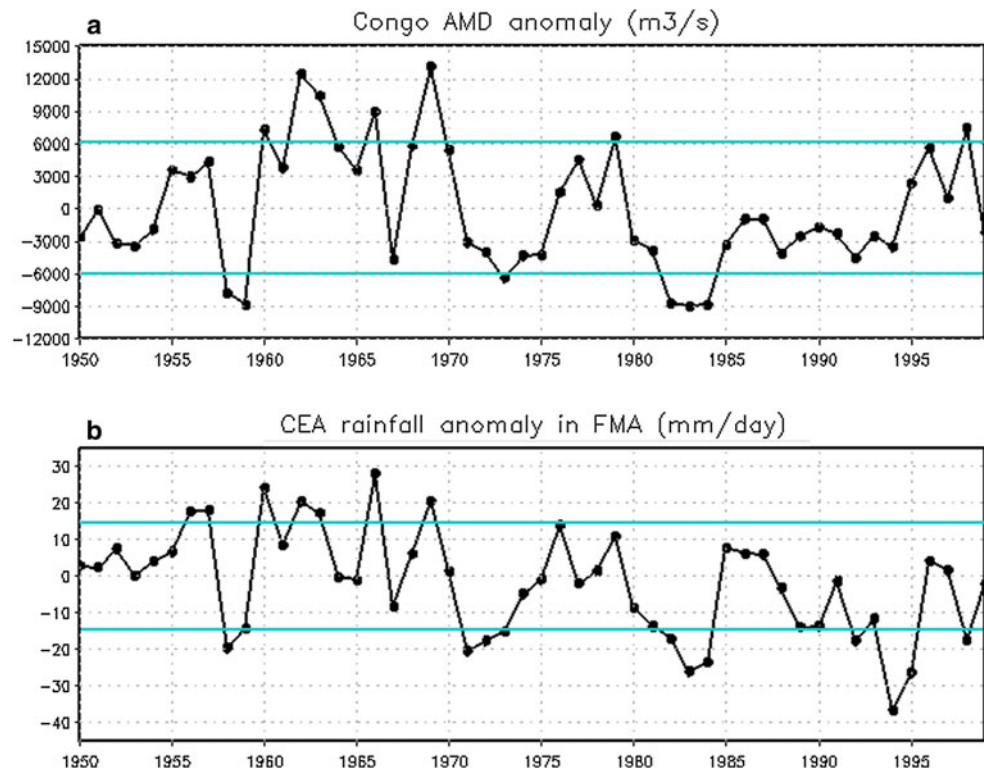
Boyer Montégut et al. 2004). Mixed layer was used in this study to calculate the SST variations induced by atmospheric fluxes. Finally, the CIGODAS global ocean reanalysis (Masina et al. 2011) were used to assess the role of stratification on SSTAs.

After a preliminary investigation which links SSTs in tropical oceans with rainfall in CEA, the main analysis concentrates on the relationship between freshwater and ocean salinity and temperature. We performed a composite analysis over 50-years observations (1950–1999) of the Congo River secondary peak discharge occurring in April–May (AM), whose annual series is shown in Fig. 3.

Within the time-series chosen we considered two different cases. We selected both the years with highly pronounced peak discharges, (secondary peak discharge anomaly exceeds one standard deviation, hereafter AMD+), and the years characterized by low peak discharges (negative anomalies are below one standard deviation, hereafter AMD–). SST and SSS fields in the following summer were averaged over the selected years.

In order to endorse our hypothesis about the influence of Congo River FWD on SST in the Gulf of Guinea, we wanted to discard possible other causes of temperature anomalies. First, we calculated SST composites in relation

Fig. 3 **a** AM Congo River discharge anomaly (m^3/s) and **b** FMA Central Equatorial Africa precipitation anomaly (mm/day). Blue straight lines indicate standard deviations



to opposite regimes of the net input of freshwater (i.e. precipitation minus evaporation, P-E) over the Gulf, and then we extended composite analysis to atmospheric fluxes and surface winds as well.

3 Description of the region

3.1 Seasonal cycle

SST variability in EEA is dominated by the annual cycle (Xie and Carton 2004). Temperatures reach their maximum during boreal spring (Fig. 2a, b), when solar radiation is the highest and winds are the weakest. In this season the SST exceeds $28\text{ }^{\circ}\text{C}$ in the whole area of the Gulf. Near the end of the season, trade winds along the equator intensify, creating a zonal pressure gradient in the ocean resulting in a thermocline uplifting. Driven by southerly winds, coastal upwelling starts and a decline of SSTs follows: the so-called equatorial cold-tongue develops in late spring and persists through September, with SSTs around $23\text{ }^{\circ}\text{C}$ in August. Besides, boreal summer turns out to be the season with the highest inter-annual variability (Joly and Voldoire 2009), since the drop in SST does not occur at the same time and intensity every year (Marin et al. 2009).

During the summer, north-east and south-east trade winds meet along ITCZ (not shown), where a convective rain band located $5\text{--}10^{\circ}\text{N}$ over the Atlantic develops (Fig. 2b). This area is characterized by the minimum

seasonal variance of SST and the highest vertical displacement of the thermocline (Houghton 1991). Over the continent, the rain band mostly follows the seasonal course, reaching its northernmost (southernmost) position in JAS (DJF) (Biasutti et al. 2003).

Boreal summer is the rainy season in Sahel, a region longitudinally crossing Africa between 5° and 18°N . In autumn the rain belt starts moving southward and discharges large amounts of rain over Central Equatorial Africa, pinpointed by the index CEA ($\text{lon} = 15^{\circ}\text{E}$, 32°E ; $\text{lat} = 12^{\circ}\text{S}$, 7°N) shown in Fig. 1. Precipitation falling in CEA is well correlated with Congo River discharge, since the region encloses almost perfectly the boundaries of its watershed. Lagged about two months after rainfall maximum, Congo River exhibits a main peak discharge in December (Fig. 2a). The second peak discharge occurs in May, driven by precipitation over the catchment during FMA, which follows the northward movement of the ITCZ (Fig. 2b). Early summer and late winter are the driest seasons in CEA, followed by river runoff minima in March and August. Despite the seasonal modulation, discharge at Brazzaville river station, is very high throughout the whole year: mean annual discharge is about $40,000\text{ m}^3/\text{s}$ and monthly means never go below $30,000\text{ m}^3/\text{s}$.

3.2 CEA rainfall variability and tropical SST

In the period 1950–1999, Congo River secondary peak discharge shows decadal or near decadal oscillations

(Fig. 3a) associated with rainfall variability in CEA. This feature was already pointed out by a few studies (e.g. Moron et al. 1995; Camberlin et al. 2001). The presence of the world's second most extensive equatorial forest delays the ingress of rain in the river system, so that average peak discharges are about two month-lagged with respect to precipitation maxima (Fig. 2a). Consequently, rainfall falling in late winter–early spring (February–March–April, hereafter FMA) turns out to have the largest covariance with Congo secondary peak discharge (Fig. 3a, b).

We performed a composite analysis to examine the role played by SST in the Tropics on CEA rainfall variability in FMA. We determined the wettest (driest) seasons in the region, selecting years in which precipitation anomalies in CEA exceed one (minus one) standard deviation. We obtained seven wet and ten dry FMA seasons (Table 1), and we calculated tropical SST composites in the same season and in the previous (November–December–January).

Anomalies in the north tropical Atlantic induce a wet spring season in CEA (Fig. 4a). SSTs are warmer than average in the Caribbean Sea since the end of the fall, and anomalies grow over time, becoming intense in the spring and spreading out all over the north tropical Atlantic. In south Atlantic and the Gulf of Guinea instead, SSTAs are negligible. Warm waters characterize the north tropical Pacific, in particular the central part, while western Pacific and part of the Indian Ocean have cold anomalies that tend to reduce as the season goes by.

In the dry composite (Fig. 4b), south Atlantic develops warm anomalies starting from the winter, especially close to South America, while anomalies are insignificant in the Gulf of Guinea. A remarkable ENSO pattern anomaly develops in the winter too, mostly driven by the strong El Niño episodes occurred in 1982–1983 and 1997–1998 with the contribution of 1957–1958 and 1994–1995 events. Balas et al. (2007), who undertook a similar composite analysis dividing central Africa in five sub-regions, suggest that different areas in CEA are influenced by distinct

sectors of the Pacific. On the other hand, the non-linearity with the wet composite suggests that ENSO is not the only forcing mode of rainfall variability in equatorial Africa. In the Indian Ocean and Indonesia the sign of SSTAs is reversed with respect to the wet case, with warm anomalies more significant and persisting over time.

4 Results

4.1 Direct effect induced by river discharge

The basic hypothesis of this work consists in the relationship between the Congo River discharge and SSS along the coast of central Africa, which would affect SST and expand to the Gulf of Guinea. A lagged correlation analysis performed on the whole year, and not only on the secondary peak discharge, shows that discharge from the Congo River is significantly correlated with salinity and temperature in the EEA (Fig. 5). Salinity (Fig. 5a, d) shows high sensitivity to Congo River discharge, and the fact that higher correlation are found off the coasts indicates that many other rivers benefit of precipitation on CEA and contiguous areas.

Significant correlations between Congo discharge and SST along the coast, which eventually propagate to the Gulf of Guinea, seem to follow salinity anomalies (Fig. 5e–h). Table 2 gives a numeric overview of the correlation at the outlet of the Congo River (Congo Mouth Index, CMI, lon = 10°E, 12°E; lat = 7°S, 5°S) and in the eastern equatorial Atlantic (Index EEAI, lon = 12°W, 10°E; lat = 10°S, 5°N), shown in Fig. 6. Each monthly discharge anomaly was associated with SSS and SST anomalies occurring before (one and two months), at the same time, and lagged up to four months. Correlations with salinity are larger than with temperature, and higher values, although still small due to the wide domain averaged and the very long time series (600 months), are usually founded at lag 0 at the Congo outlet, while they are one-two months delayed in the Gulf of Guinea.

Limiting our analysis to the secondary peak discharge, we notice that, during the period 1950–1999, river runoff exceeds the one standard deviation threshold (Fig. 3a) seven times. Between 1960 and 1970, a period of exceptional rainfall hit the Congo drainage basin (Sanga-Ngoie and Fukuyama 1996) and five of the outstanding peak discharge anomalies occur in this decade. A drier cycle starts at the beginning of the seventies and appears to last about 20–25 years. Congo shows high secondary peak discharge only once (1979) until mid-nineties, when the dry period seems to terminate and positive anomalies become more frequent (see also Laraque et al. 2001): year 1998, in fact, turn out to be AMD+.

Table 1 Wettest and driest FMA seasons in Central Equatorial Africa (CEA) for the period 1950–1999

Wettest years	Driest years
1956	1958
1957	1971
1960	1972
1962	1982
1963	1983
1966	1984
1969	1992
	1994
	1995
	1998

Data provided by CRU

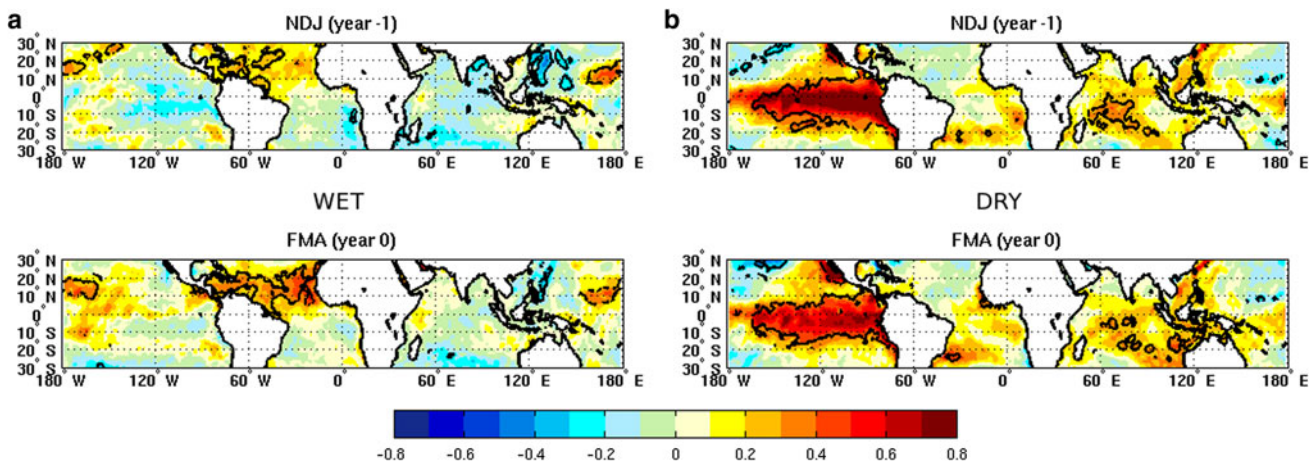


Fig. 4 Tropical Ocean SST anomalies (°C) in (a) the five wettest and (b) the five driest (*right panel*) FMA seasons in CEA. *Black solid lines* represent the 95 % confidence after bootstrap test

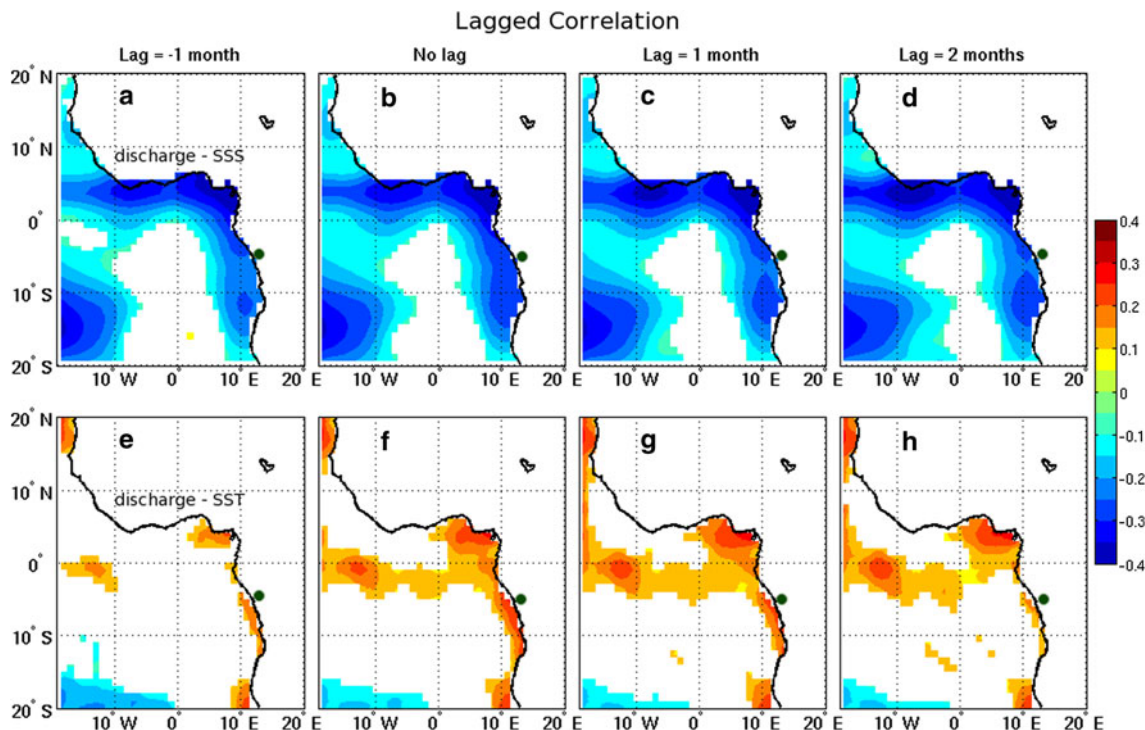


Fig. 5 Correlation between river discharge and SSS (*top panel*) and river discharge and SST (*bottom panel*). Shaded values are significant at the 95 % confidence level (*t* test)

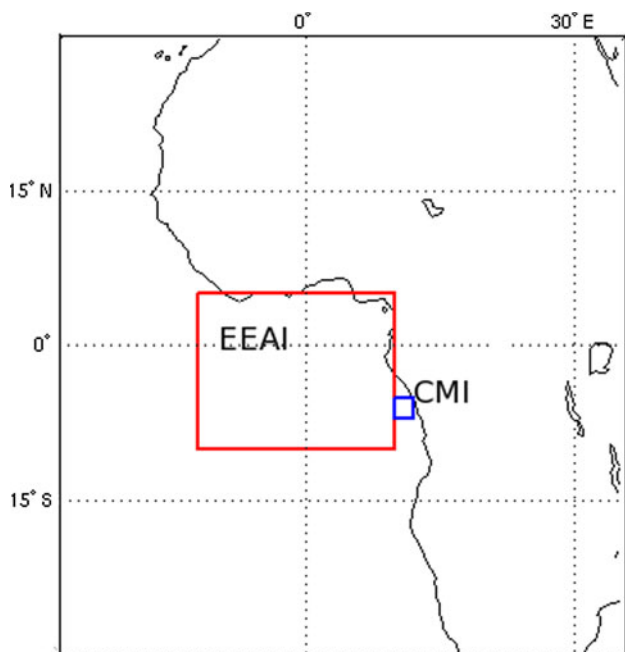
Salinity is the ocean variable mainly affected by river discharge variability: river water freshen the upper layers of the ocean, creating a strongly stratified plume, which is transported through advection. At the beginning of AMD+ summers, a wide SSS negative anomaly develops along the eastern coast of Africa in correspondence of the Congo mouth (Fig. 7a), in response to the abnormal amount of freshwater. Negative SSS anomalies are present in the Gulf of Guinea through the summer, with the largest significant deviations straddling the Equator.

In AMD+ years, SSTs in the Gulf are warmer than average during the entire summer season (Fig. 8a–d). In April, Congo River starts discharging its anomalous freshwater flux into the Atlantic Ocean, and in May a warm SSTA appears in correspondence of the river mouth (Fig. 8a–d). The anomaly propagates towards the EEA advected by surface currents. Near the coast, the plume first spread WNW (Vangriesheim et al. 2009), and keeps flowing to the west offshore as indicated by data from drifting buoys (Hansen and Poulain 1996, not shown).

Table 2 Lagged correlation between Congo River discharge and SSS at the Congo outlet (CMI index) and in the Eastern Equatorial Atlantic (EEAI index), and between Congo River discharge and SST at CMI and EEAI

	SSSA CMI	SSSA EEAI	SSTA CMI	SSTA EEAI
Lag -2	-0.13	-0.12*	0.08	0
Lag -1	-0.22**	-0.16*	0.15*	0.03
Lag 0	-0.26**	-0.20**	0.21**	0.10
Lag 1	-0.24**	-0.21**	0.19**	0.15**
Lag 2	-0.23**	-0.22**	0.12*	0.12*
Lag 3	-0.19**	-0.18**	0.10	0.12*
Lag 4	-0.16*	-0.17*	0.08	0.11

Each monthly discharge within the period of analysis (1950–1999) was correlated with SSS and SST measured from two month before (lag -2) to four months later (lag 4). Double (single) star indicates 95 % (90 %) significance, obtained through a Student *t* test

**Fig. 6** Eastern Equatorial Atlantic (EEAI) and Congo Mouth (CMI) indexes

In the second half of the last century, the Congo secondary peak discharge is lower than the standard deviation threshold six times. Four of these cases occur during the relatively dry period 70-90, and two before the wet 1960s decade (Fig. 3a).

Composites of SSS in the EEA show that late spring and the entire summer are characterized by positive anomalies when Congo spring discharge is low. Most likely, the excess of saline water is explained by the substantial decrease of freshwater discharged by the river (Fig. 7e–h). In fact, the largest anomalies of salinity occur along the African coast, in particular in proximity of the Congo mouth and in the Gulf, where many other large rivers (e.g. Sanaga, Ogooue) discharge their lower amount of freshwater. Again, the deviation from the mean persists through

the summer and invades a large region in the Gulf of Guinea.

Following low freshwater incomes, in May a negative SSTA develops along the African western coast, with a minimum near the river outlet (Fig. 8e). This cold tongue grows and expands over the Gulf of Guinea in June, exceeding -0.5 °C anomaly, and persists through July, when the significance of SST cold anomalies fades away (Fig. 8f–h).

The temperature increase in AMD+ can be explained by the accumulation of vast amounts of freshwater in the upper layers of the ocean, which increases stratification. Cold anomalies, instead, appear when the discharge from Congo River is low and salinity surplus prevents stratification. Similarly to Park et al. (2011), who analyzed the impact Chang Jiang River FWD on the East China Sea, we show year to year variation of SSS, SST and mixed layer depth anomalies from CIGODAS reanalysis, used as an indicator for stratification, in the CMI domain for the AM season (Fig. 9a). Generally, salinity anomalies are positively correlated to vertical mixing, which means that vertical mixing is inhibited in the event of discharge of large amounts of freshwater. On the other hand, SSTs are often anti-correlated to the depth of mixed layer, which means that warm biases occur with stratification at the top of the ocean. Figure 9b, c shows a zoom of the Congo mouth region, with a spatial representation of the opposite association between stratification and salinity, and stratification and temperature. An increase (decrease) in stratification caused by negative (positive) salinity anomalies, leads to inhibition of vertical mixing (that is reduction of the mixed layer depth) with less water exchange between the ocean surface and lower layers. This eventually turns into warm (cold) anomalies at the surface.

The linear regression between SST and mixed layer depth shown in Fig. 10 reinforces this hypothesis. In AM, temperature at the Congo mouth decreases by 0.21 °C per meter of mixed layer deepening.

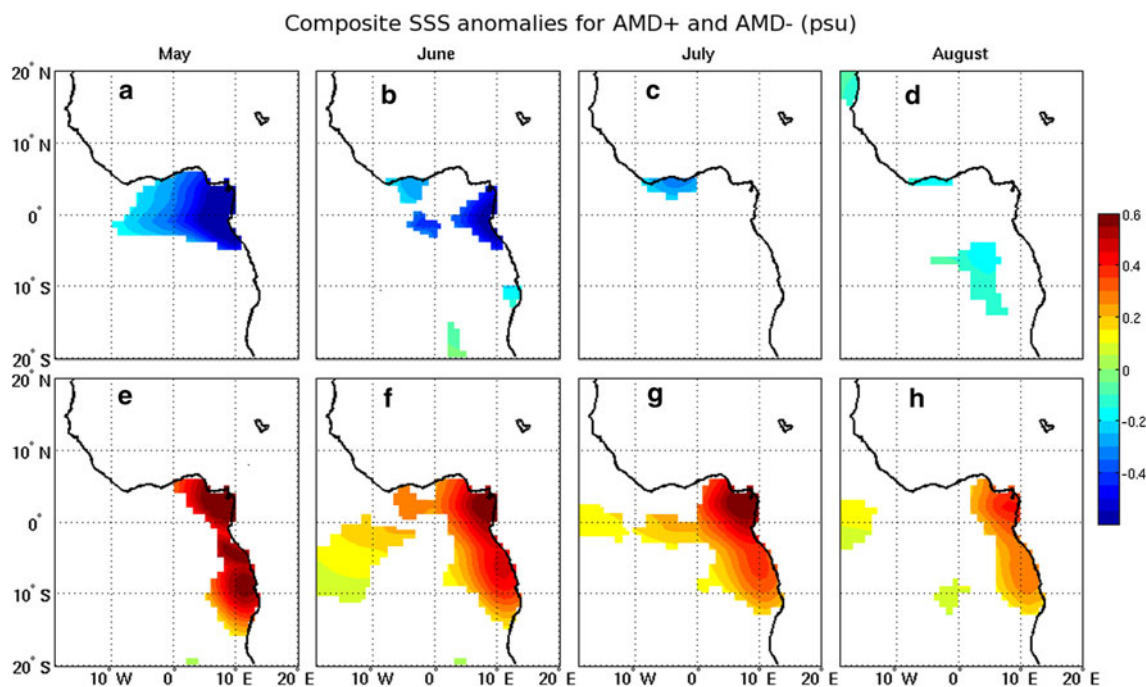


Fig. 7 Composite of sea surface salinity anomalies (psu) in **a** AMD+ years and **b** AMD- years. Shaded regions indicate anomalies significant at the 95 % level (bootstrap technique)

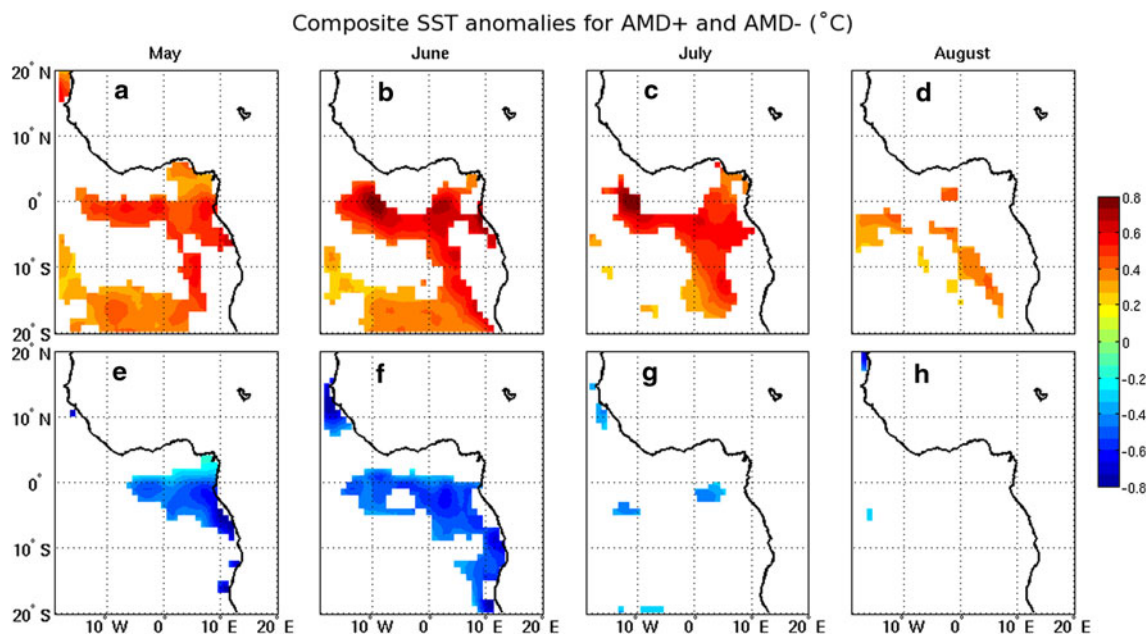


Fig. 8 The same as Fig. 7 for sea surface temperatures (°C)

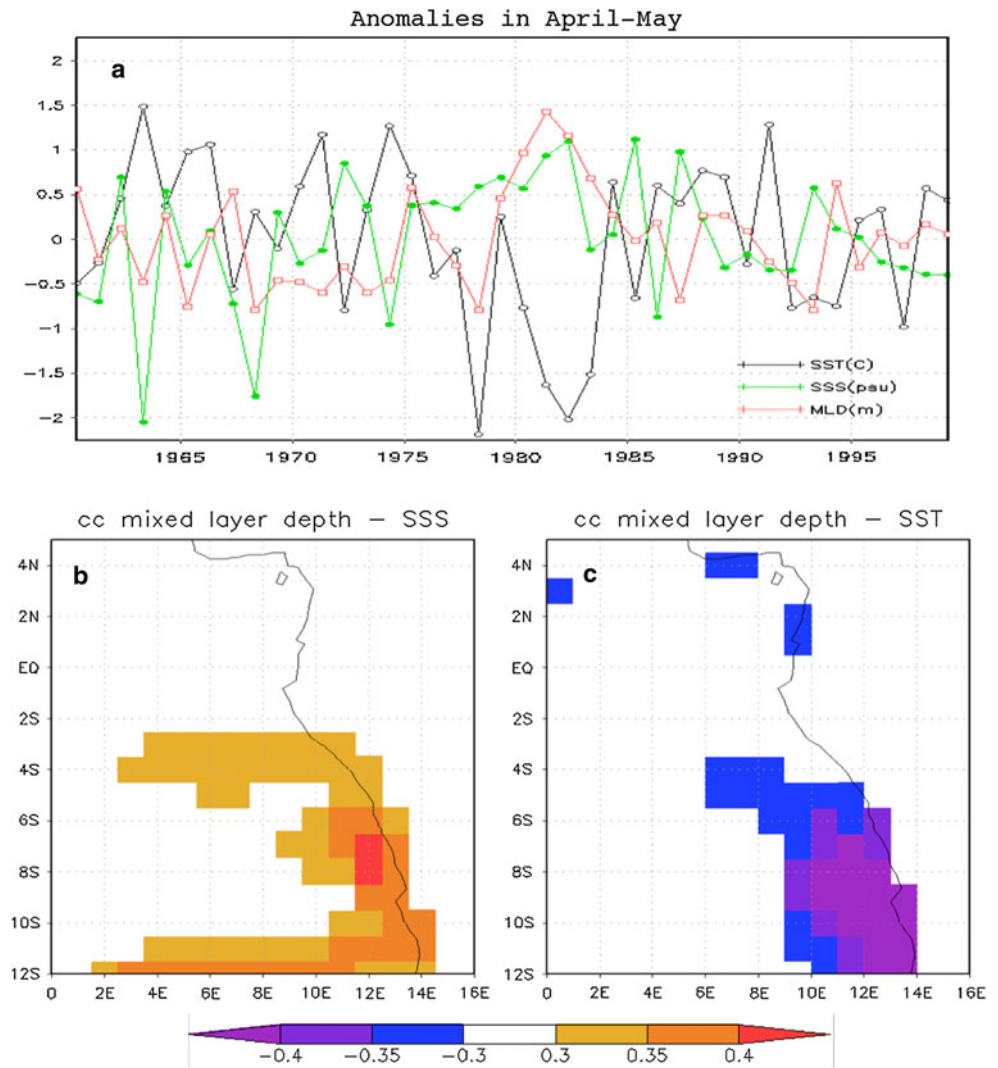
4.2 Role of the net input of freshwater

We saw that freshwater anomalies in the EEA can be due to atypical flux advected from the Congo and other river mouths. However, intense local rainfall anomalies may have the same effect. Therefore, here we try to discriminate between the role of river discharge and the net freshwater

input, i.e. the difference between precipitation and evaporation (P-E), on the SSTAs.

To this aim, we used the index EEAI of P-E over the Eastern Equatorial Atlantic, defined as the freshwater anomaly averaged over the region. We used the GPCP and OAFux datasets for precipitation and evaporation respectively, and we identified years characterized by P-E

Fig. 9 **a** Year to year variability of mixed layer depth (red), SSS (green) and SST (black) at the Congo mouth (CMI index) in May. **b** Correlation between mixed layer depth at CMI and SSS and **c** between mixed layer depth at CMI and SST. Shaded values are significant at 95 % (Student *t* test)



anomalies exceeding the threshold of ± 1 standard deviation. Since GPCP is available only since 1979, we prolonged our analysis through 2006. In this way we could identify a larger number of SST composites, increasing the statistical robustness of our analysis.

P-E positive anomalies in spring (April and May) cross the threshold of $+1$ standard deviation in five occurrences (1984, 1995, 1996, 1999, 2002, not shown), and the surface temperatures measured in the Gulf in the following months are much warmer than usual (Fig. 11a–d). Then, abnormally large freshwater inflow acts to heat the ocean in the area. Opposite is the case of dry springs in EEAI, which take place in 1987, 1992, 1993 and 1997: in the following summer SST composites show intense negative anomalies (Fig. 11e–h).

In the period available for GPCP, AMD+ occurs in 1979, 1996 and 1998, and only the second one is characterized by large freshwater input also over the Gulf. Springs 1982, 1983 and 1984 are marked by low Congo River runoff, and none of them is a dry spring in EEAI.

Despite the small number of samples, we can state that there is no evidence of an interconnection between Congo discharge and rainfall anomalies over EEA, as it is confirmed by overlapping the two time series (Fig. 11). On the other hand, freshwater anomalies generated by river runoff produce the same effect as the ones originated by P-E.

In order to evaluate the SST variability explained by the two sources of spring freshwater, a lagged regression analysis was set, and results are shown in Table 3. The portion of SST variability associated with P-E flux over EEA is much larger than the one explained by the river discharge, which turns out to be only 6 % in June. However, although a clear freshwater effect is not significant in most of the years, extreme seasons have a remarkable impact on the EEA temperatures, and this effect is obviously more pronounced in the event of an excess of freshwater input. In fact, likewise the SST composites to spring river discharge, the response of SST to anomalous precipitation is not linear, with warm anomalies much more pronounced than cold ones.

Fig. 10 Linear regression between mixed layer depth and SST in the CMI domain. A 1 meter deepening of the mixed layer is translated in 0.21 °C decrease in SST

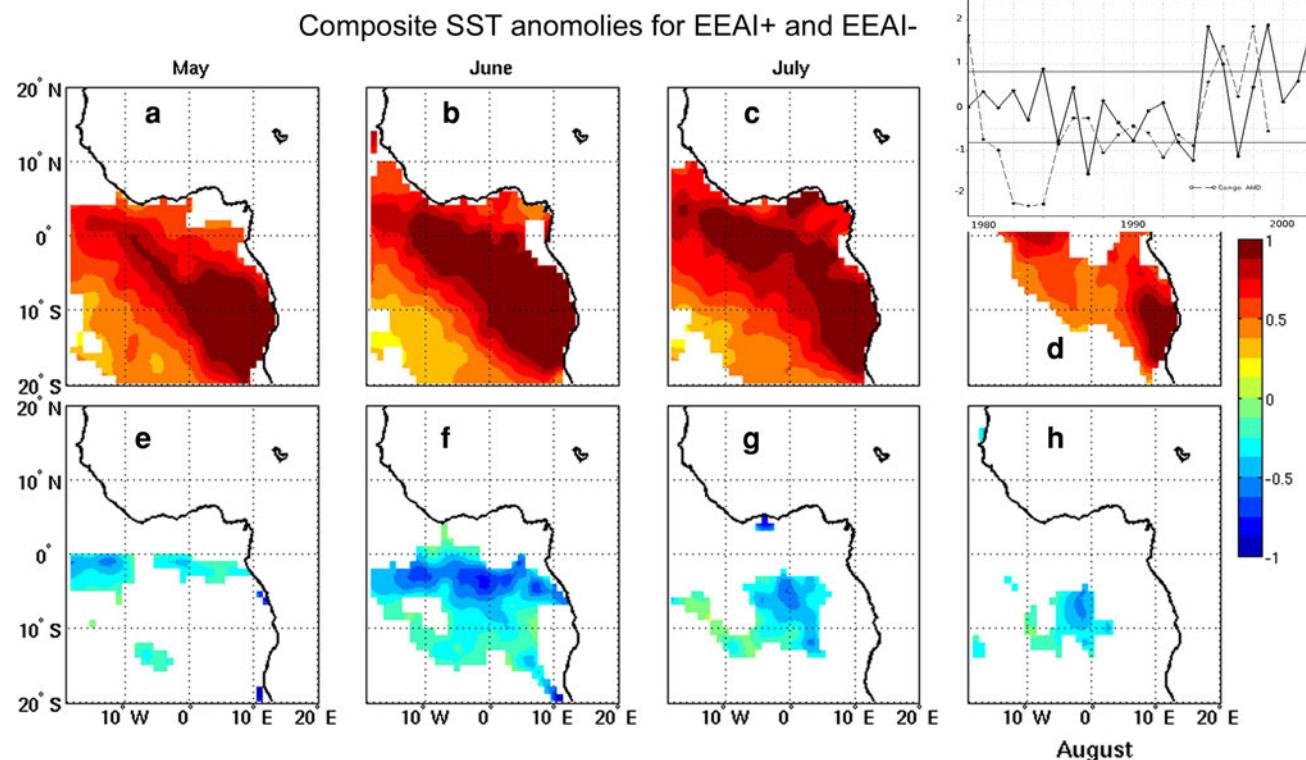
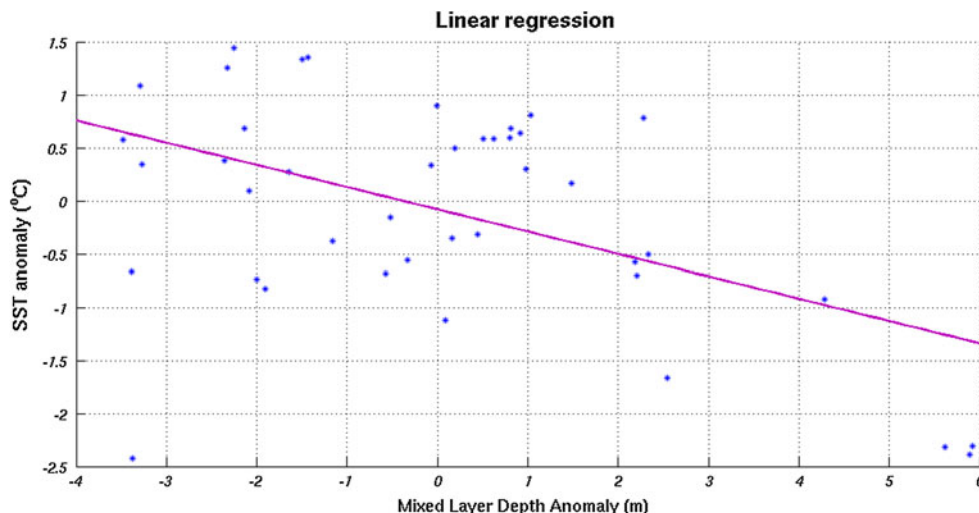


Fig. 11 SST composite anomalies (°C) in April–May seasons characterized by (a–d) large and (e–h) low net input of freshwater (P–E) over EEAI. Shaded areas indicate anomalies significant at the 95 % level (Bootstrap technique). Embedded, at the top right, the AM

time series of P–E anomaly over EEAI (solid line). The thinner dashed line indicates the anomaly of Congo River discharge for the same period

4.3 Role of heat fluxes

Another possible mechanism affecting the sea surface temperature is the heat exchange between the atmosphere and the ocean. Surface net radiation, latent and sensible heat fluxes act directly on the ocean surface modifying its temperature. In order to clarify the possible role of

atmospheric fluxes on EEA warming (cooling), we calculated composites in AMD+ (AMD–).

Figure 12a–d shows ERA40 total fluxes at the surface in AMD+. In May, a cold anomaly starts developing in the western region, widening and expanding westward in the succeeding months. In June and July, the atmosphere heats the northernmost part of the Gulf of Guinea, while the

Table 3 SST variance explained (through linear regression technique) by P-E over EEAI by Congo river discharge, P-E over EEAI, heat fluxes over EEAI, surface winds along the south Atlantic coast of Africa (0°–30°S)

	Congo discharge (%)	P-E in EEAI (%)	Heat fluxes in EEAI (%)	Surface winds (%)
SST May	5	17	7	39
SST June	6	15	7	31
SST July	5	10	6	28
SST August	2	8	6	21

southern region gets cooler. It is interesting to note that the warmest SSTAs in AMD+ years occur south of the Equator (Fig. 8a–d), which is in contrast with the flux pattern anomalies shown in Fig. 11a.

The reverse structure takes place during the summer in AMD– (Fig. 12e–h), with atmospheric fluxes cooling the northern area of the Gulf and heating the southern part. At the same time, SST composites show that south EEAI is subject to a cold anomaly, while the northern sector is warmer than average (Fig. 8d–h). Also, the cold anomaly near the Congo mouth is not supported by analogous fluxes anomaly.

We made a simple and rough estimate of the temperature anomalies associated with atmospheric fluxes, to evaluate how much of the SSTA signal can be explained by the fluxes anomalies. We made use of the Eastern Equatorial Atlantic Index (EEAI) and the Congo Mouth index (CMI) (Fig. 6). In these domains, composites of sensible heat, latent heat and surface net radiation anomalies in AMD+ and AMD– were calculated and summed up. Then, the corresponding SSTAs were obtained through the relation:

$$\Delta T = \frac{Q_{fl}}{m \cdot c_p} = \frac{Q_{fl}}{V \cdot \rho_{H_2O} \cdot c_p} \quad (1)$$

ΔT is the deviation from the mean SST, Q_{fl} is the heat flow required to change the water temperature, c_p is specific heat at constant pressure, m is the mass of water. V (where $V = A \times h$) is the volume of water heated by the atmosphere, defined as the depth of the water layer warmed up by the heat flux (h) per unit area (A).

On first approximation, h was chosen as the monthly mixed layer depth given that mixed layer is defined as a fully turbulent region of quasi-isopycnal and isothermal water (Mellor and Durbin 1975). de Boyer Montégut et al. (2004) identify the optimal density criterion in 0.03 kg/m³ difference from surface. In the Gulf of Guinea, mean annual mixed layer depth is about 20 m (Fig. 13a), but it is shallower in late spring and summer (Fig. 13b). The mixed layer is about 12–15 meters deep near the Congo mouth during the summer.

Figure 14a shows a comparison of monthly HadSST2 anomalies (solid lines) and SSTA derived by ERA40 fluxes (bars), using Eq. (1), in EEAI. Here we show temperatures

for the month of April as well, to take into account possible delayed effects of the fluxes on SST. In AMD+ years (red graphs), the ocean surface is warmer than normal through the end of the summer, with the largest anomaly in June (about 0.4 °C). At the same time, the atmospheric fluxes drive cold anomalies, with a minimum in July. In AMD– years (blue graphs) as well total fluxes do not look sufficient to explain negative SSTA in the EEAI. In May and June the Gulf gets much colder than average (around 0.3 °C), while fluxes still induce positive or zero temperature anomalies. In July and August the cold anomaly fades away and so temperature anomaly induced by the atmosphere.

Figure 14b shows the same analysis performed in CMI. In AMD+ years, the ocean region contiguous to the Congo River mouth records large positive anomalies (about 0.5 °C) through early summer, which rapidly decrease to not significant values. Heat fluxes induce only a minor part of this warming in the spring, while in the summer their effect would drive negative SSTAs. In AMD–, surface temperature observed in CMI are colder than average till June, with a minimum peak in May, while fluxes would tend to warm the ocean. Their effect is likely responsible of the warming that verifies at the end of the summer.

4.4 Role of surface winds

As mentioned above, the area of the study is characterized by coastal upwelling. Southerly winds blowing along the coast drive Ekman transport, through which water is moved away from the coast and replaced by colder water that wells up from below. When coastal wind blows stronger, its stress on the ocean is amplified and surface water cools off as a consequence of the entrainment, while weaker winds have opposite effect (e.g. Marin et al. 2009). De Coëtlogon et al. (2010) have found wind stress to be the first mode of variability in the Gulf of Guinea in boreal spring and summer, while Richter et al. (2012), state that deficient easterly wind stress in MAM is the primary reason for the severe JJA equatorial SST biases in a fully coupled model experiment.

Table 3 shows that surface winds blowing in April and May explain large part of SST variability in the Gulf of

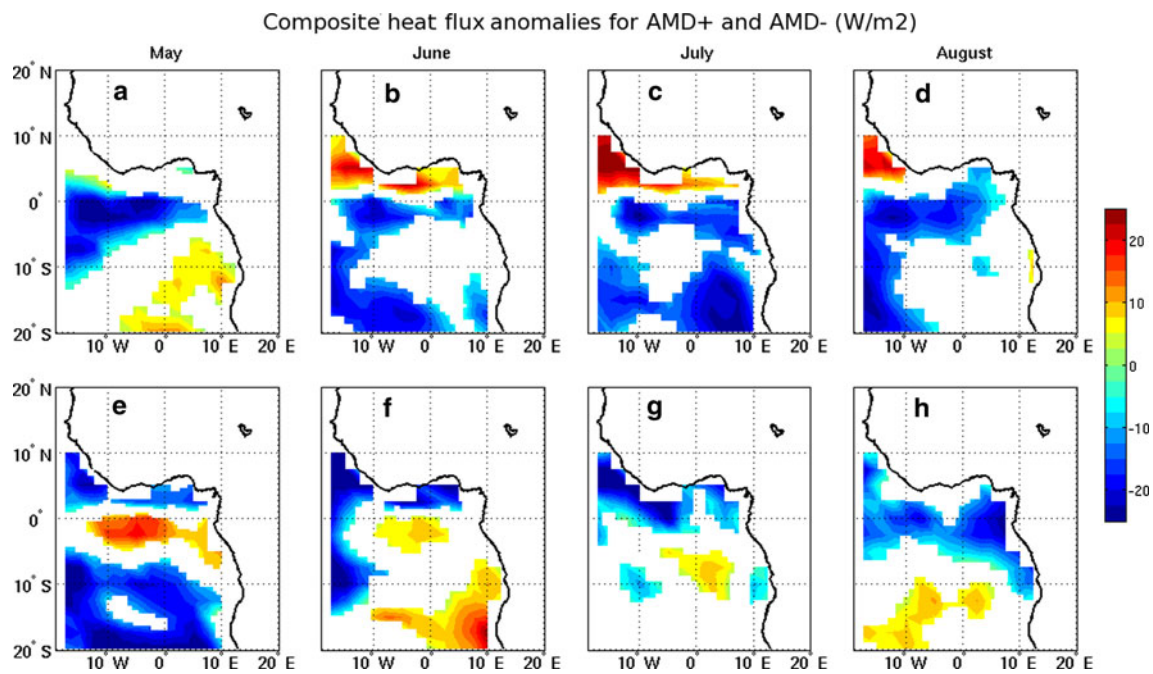


Fig. 12 Composites of total atmospheric flux anomalies (W/m^2) in (a–d) AMD+ years and (e–h) AMD– years. Shaded areas indicate anomalies significant at the 95 % level (Bootstrap technique)

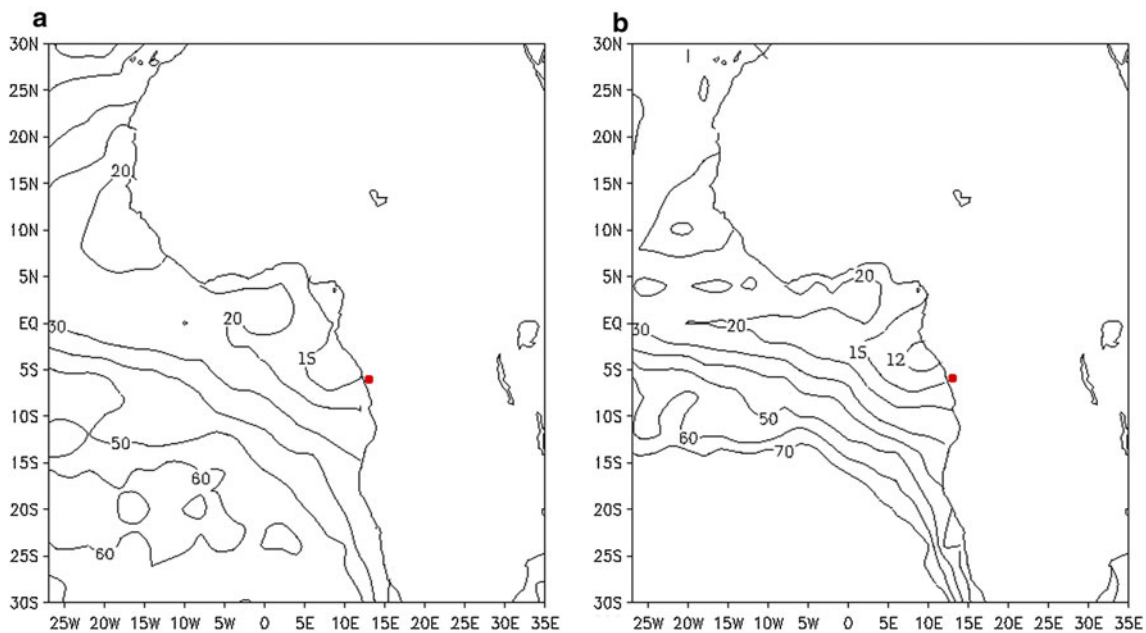


Fig. 13 a Mean annual and b summer (MJJA) (averaged 1958–2006) mixed layer depth in meters in the Eastern Tropical Atlantic region. Red circles indicate the Congo outlet

Guinea. In particular, the regression technique reveals that almost 40 % of the temperature variation in May depends on winds, and surface stress is able to explain a large portion of summer variability as well.

Yet, AMD– years are not characterized by significant positive anomalies of surface winds (Fig. 15e–h) that would

explain part of the cooling in Fig. 9e–h. In June alongshore winds are even weaker, favoring possible warm anomalies, which in fact do not occur. Negative coastal wind anomalies are instead present in AMD+ May and June (Fig. 15a–d). This could have an effect on the warm temperatures shown in Fig. 9a–d, but the area and the intensity of weaker winds do

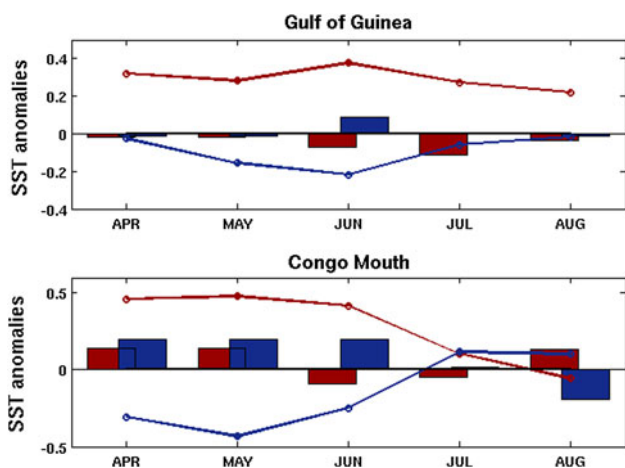


Fig. 14 Sea surface temperatures (°C) as measured by HadSST2 (solid lines) and induced by atmospheric fluxes (bar graphs) in the Gulf of Guinea and at the outflow of Congo River. Red (blue) graphs represent temperatures in AMD+ (AMD−) years

not seem to be able to explain such a consistent SST warm anomaly in the Gulf of Guinea. Besides, wind anomalies have a direct influence on heat fluxes, with positive

anomalies of the former leading to negative of the latter (Fig. 12). Heat fluxes though are not responsible for SST changes, as we explained in Sect. 4.3.

5 Discussion and conclusion

In this study we investigate the chain of feedbacks between Congo River discharge, surface salinity and SST in the Eastern Tropical Atlantic. In particular, we focus on the secondary peak discharge (i.e., the peak that occurs in May, during the equatorial rainbelt migration towards north). Results show the active role played by freshwater in altering the interannual variability of Eastern Equatorial Atlantic.

An excess of freshwater flow, occurring when Congo secondary peak discharge is well above the average (AMD+), reduces the amount of salinity in the region off the river mouth and part of the Gulf of Guinea. Conversely, scarce springtime river discharge (AMD−) leads to negative salinity anomalies. When a surplus of freshwater occurs, the ocean surface warms up, and positive SSTAs

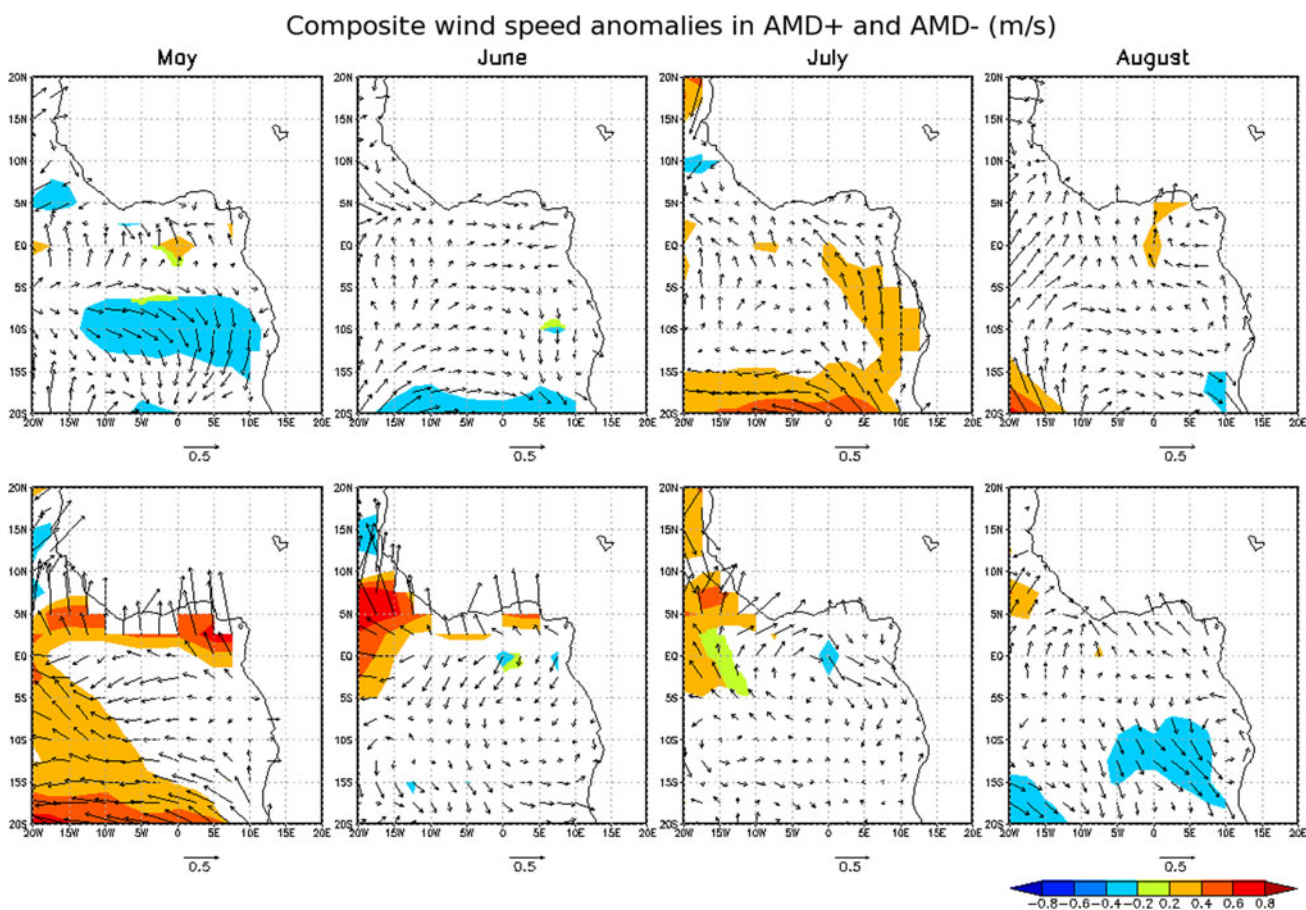


Fig. 15 Composites of surface winds in (a–d) AMD+ years and (e–h) AMD− years. Shaded areas indicate anomalies significant at the 95 % level (Bootstrap technique), while vectors represent the total wind speed and direction anomalies

arise in EEA, while temperature anomalies are reversed in the event of low FWD. The temporal and spatial distribution of the anomalies is different in the two cases, disclosing the non-linearity of the effect of low and high river discharge on the SST in the Gulf. This is most likely due to the formation of a long-lasting barrier layer in case of large freshwater income, with inhibition of vertical mixing between the surface and the cold thermocline. This hypothesis is in line with previous studies performed in other regions characterized by the presence of large river mouths. In the event of low discharge instead, the excess of salinity does not change much the vertical density stratification, which is mainly determined by the temperature, and anomalies are less pronounced. Only 6 % of the EEA SST variability is generally explained by the Congo River, but the impact of its spring freshwater discharge in exceptionally wet or dry years is remarkable.

Some analyses were performed to verify the hypothesis that SST alteration is actually induced by the outflow of Congo River. First we evaluated the effect of the major source of freshwater flow in the area, that is precipitation. Ocean is anomalously warm in seasons characterized by heavy precipitation over the Gulf, while dry years seem to be associated with unusually cold SSTs. This result implies a major role of freshwater in driving SST in the Gulf of Guinea. However, wet (dry) years in the Gulf of Guinea do not coincide with anomalously high (low) Congo River discharge, and this suggests that warm (cold) anomalies in AMD+ (AMD−) years are not caused by atypical precipitation over the Gulf. Again, wet conditions lead to larger anomalies in the SSTs, strengthening the hypothesis of the formation of a barrier layer in the event of excessive freshwater income.

We also made a simple evaluation the role of heat fluxes and surface net radiation on SST in the Gulf of Guinea. This test aims to exclude that changes in the ocean thermal state are produced by atmospheric conditions only, and results appear to confirm this hypothesis. From our analysis, the intense SST drop (rise) at the end of the spring in AMD− (AMD+) years are not induced by anomalies in the fluxes exchanged with the atmosphere. The method used for this estimation has a few limitations, due to large uncertainties on the air-sea fluxes reanalysis.

The regression between coastal winds and SST revealed that surface stress has a large impact on the Gulf of Guinea interannual variability. However, speed anomalies in AMD+ and AMD− years do not seem to be crucial for the SST alteration either, both for the limited significance of their anomalies and because surface winds directly affect fluxes, whose anomalies turned out to be irrelevant to SST changes.

This study was performed considering observational and reanalysis data only, therefore, due to the limitations of these

datasets, many variables that would be useful to our analysis may not be taken into consideration. Vertical velocities and diffusion are not available in observations, while temperature and salinity profiles are sparse and discontinuous. Hence, this study represents a first step, where some work hypotheses and methodologies were verified starting from observational datasets. A more comprehensive and in depth analysis of the feedbacks between river discharge, salinity and sea temperature will be performed by following works, which will take into account the effect of FWD on ocean features through the use of numerical model experiments.

Finally, this study takes into account continental FWD, a variable often neglected in studies about tropical Atlantic. Not only may such a feature be an important factor of variability, but also it should be taken into account in the assessment and correction of the SST bias along the south Atlantic coast of Africa, which affect the large majority most of the fully coupled climate models (see e.g. Large and Danabasoglu 2006).

Acknowledgments The authors acknowledge the support of the Italian Scientists and Scholars in North America Foundation (ISSNAF), through a fellowship sponsored by Ministero dell'Ambiente e della Tutela del Territorio e del Mare, Direzione Generale per la Ricerca Ambientale e lo Sviluppo, Italy. They acknowledge the support of the project Climafrika, in the Seventh Framework Program of the European Union, for the latest stage of the work. Stefano Matera is thankful to Alessio Bellucci and Giuseppe Zappa for the useful conversation on oceanography and statistics, and Enrico Scoccimarro for the technical support. The author is also grateful to Joe Tribbia, Bill Large, and the whole staff of the National Center for Atmospheric Researches (Boulder, CO), who make facilities available during part of the manuscript drafting. Finally, sincere thanks go to all the reviewers, whose precious contribution helped to improve and complete this manuscript.

References

- Adler RF, Huffman GJ, Chang A, Ferraro R, Xie P, Janowiak J, Rudolf B, Schneider U, Curtis S, Bolvin D, Gruber A, Susskind J, Arkin P (2003) The version 2 global precipitation climatology project (GPCP) monthly precipitation analysis (1979-present). *J Hydrometeorol* 4:1147–1167
- Balas N, Nicholson SE, Klotter D (2007) The relationship of rainfall variability in West Central Africa to sea-surface temperature fluctuations. *Int J Climatol* 27(10):1335–1349
- Biasutti M, Battisti DS, Sarachik ES (2003) The annual cycle over the tropical atlantic, South America, and Africa. *J Clim* 16:2491–2508
- Breugem WP, Hazeleger W, Haarsma RJ (2007) Mechanisms of northern tropical Atlantic variability and response to CO2 doubling. *J Clim* 20(11):2691–2705
- Breugem WP, Chang P, Jang CJ, Mignot J, Hazeleger W (2008) Barrier layers and Tropical Atlantic SST biases in coupled GCMs. *Tellus* 60A:885–897
- Camberlin P, Janicot S, Poccars I (2001) Seasonality and atmospheric dynamics of the teleconnection between African rainfall and tropical sea surface temperature: Atlantic vs ENSO. *Int J Climatol* 21:973–1005

- Carton JA (1991) Effect of seasonal surface freshwater flux on sea surface temperature in the Tropical Atlantic Ocean. *J Geophys Res* 96(C7):12593–12598
- Chamarthi S, Ram PS (2009) Role of freshwater discharge from rivers on oceanic features in the Northwestern Bay of Bengal. *MarGeod* 32(1):64–76
- Chamarthi S, Ram PS, Josyula L (2008) Effect of river discharge on Bay of Bengal circulation. *Mar Geod* 31(3):160–168
- Covey D, Hastenrath S (1978) The Pacific El Niño phenomenon in the Atlantic sector. *Mon Weather Rev* 106:1280–1287
- Davey MK, Huddleston M, Sperber KR, Braconnot P, Bryan F, Chen D, Colman RA, Cooper C, Cubasch U, Delecluse P, DeWitt D, Fairhead L, Flato G, Gordon C, Hogan T, Ji M, Kimoto M, Kitoh A, Knutson TR, Latif M, Le Treut H, Li T, Manabe S, Mechoso CR, Meehl GA, Power SB, Roeckner E, Terray L, Vintzileos A, Voss R, Wang B, Washington WM, Yoshikawa I, Yu JY, Yukimoto S, Zebiak SE (2002) STOIC: a study of coupled model climatology and variability in tropical ocean regions. *Clim Dyn* 18:403–420
- de Boyer Montégut C, Madec G, Fischer AS, Lazar A, Iudicone D (2004) Mixed layer depth over the global ocean: an examination of profile data and a profile-based climatology. *J Geophys Res* 109:C12003. doi:10.1029/2004JC002378
- De Coëtlogon G, Janicot S, Lazar A (2010) Intraseasonal variability of the ocean–atmosphere coupling in the Gulf of Guinea during boreal spring and summer. *Q J R Meteorol Soc* 136:426–441
- Dessier A, Donguy JR (1994) The sea surface salinity in the tropical Atlantic between 10 S and 30 N: seasonal and interannual variations (1977–1989). *Deep Sea Res Part I Oceanogr Res Pap* 41(1):81–100
- Ffield A (2007) Amazon and Orinoco River plumes and NBC rings: bystanders or participants in hurricane events? *J Clim* 20(2):316–333
- Giannini A, Saravanan R, Chang P (2005) Dynamics of the boreal summer African monsoon in the NSIPP1 atmospheric model. *Clim Dyn* 25:517–535
- GRDC (2011) Long-term mean monthly discharges and annual characteristics of GRDC Station/Global Runoff Data Centre. Koblenz, Germany: Federal Institute of Hydrology (BfG)
- Gu G, Adler RF (2004) Seasonal evolution and variability associated with the West African monsoon system. *J Clim* 17:3364–3377
- Hansen DV, Poulain PM (1996) Quality control and interpolations of WOCE-TOGA drifter data. *J Atmosph Ocean Tech* 13:900–909
- Hellweger FL, Gordon AL (2002) Tracing Amazon River water into the Caribbean Sea. *J Mar Res* 60(4):37–49
- Houghton R (1991) The relationship of sea surface temperature to thermocline depth at annual and interannual time scales in the tropical Atlantic Ocean. *J Geophys Res* 96 (C8):15173–5185
- Hourdin F, Musat I, Grandpeix JY, Polcher J, Guichard F, Favot F, Parquet P, Boone A, Latore JP, Redelsperger JL, Ruti PM, Dell’Aquila A, Filiberti MA, Pham M, Doval TL, Traore AK, Gallée H (2010) AMDMA-model intercomparison project. *Bull Am Meteorol Soc* 91(1):95–104
- Ingleby B, Huddleston M (2007) Quality control of ocean temperature and salinity profiles—Historical and real-time data. *J Mar Syst* 65(1–4):158–175
- Joly M, Voltaire A (2009) Role of the Gulf of Guinea in the interannual variability of the West African monsoon: what do we learn from CMP3 coupled simulation? *Int J Climatol* 30(12):1843–1856
- Laraque A, Mahe G, Orange D, Mariou B (2001) Spatiotemporal variations in hydrological regimes within Central Africa during the XXth century. *J Hydrol* 245:104–117
- Large W, Danabasoglu G (2006) Attribution and impacts of upper-ocean biases in CCSM3. *J Clim* 19:2325–2345
- Latif M, Grötzner A (2000) The equatorial Atlantic oscillation and its response to ENSO. *Clim Dyn* 16:213–218
- Lukas R, Lindstrom E (1992) The mixed layer of the western equatorial Pacific Ocean. *J Geophys Res Ocean* 96:3343–3357
- Marin F, Caniaux G, Bourles B, Giordani H, Gouriou Y, Key E (2009) Why were sea surface temperatures so different in the eastern equatorial Atlantic in June 2005 and 2006? *J Phys Oceanogr* 39(6):1416–1431
- Masina S, Di Pietro P, Storto A, Navarra A (2011) Global Ocean re-analyses for climate applications. *Dyn Atmos Oc* 52(1–2):341–366
- Mehta VM (1998) Variability of the tropical ocean surface temperatures at decadal–multidecadal timescales. Part I: the Atlantic Ocean. *J Clim* 11:2351–2375
- Mehta VM, Delworth T (1995) Decadal variability of the tropical atlantic ocean surface temperature in shipboard measurements and in a global ocean-atmosphere model. *J Clim* 8:172–190
- Mellor GL, Durbin PA (1975) Structure and dynamics of the ocean mixed layer. *J Phys Ocean* 5(4):718–728
- Mitchell TD, Jones PD (2005) An improved method of constructing a database of monthly climate observations and associated high-resolution grids. *Int J Climatol* 25(6):693–712
- Moron V, Bigot S, Roucou P (1995) Rainfall variability in subequatorial America and Africa and relationships with the main sea-surface temperature modes (1951–1990). *Int J Climatol* 15:1297–1322
- Park T, Jang CJ, Jungclaus JH, Haak H, Park W, Oh IS (2011) Effect of the Changjiang river discharge on sea surface warming in the Yellow and East China Seas in summer. *Continent Shelf Res* 31:15–22
- Philander G, Pacanowski RC (1986) The mass and heat budget in a model of the Tropical Atlantic Ocean. *J Geophys Res Oceans* 91(C12):14212–14220
- Polo I, Rodriguez-Fonseca B, Losada T, Garcia-Serrano J (2008) Tropical atlantic variability modes (1979–2002). Part I: time-evolving SST modes related to west African rainfall. *J Clim* 21(24):6457–6475
- Rayner NA, Brohan P, Parker DE, Folland CK, Kennedy JJ, Vanicek M, Ansell TJ, Tett SFB (2006) Improved analyses of changes and uncertainties in sea surface temperature measured in situ since the mid-nineteenth century: the HadSST2 dataset. *J Clim* 19(3):446–469
- Richter I, Xie SP (2008) On the origin of equatorial Atlantic biases in coupled general circulation models. *Clim Dyn* 31:587–598
- Richter I, Xie SP, Wittenberg AT, Masumoto Y (2012) Tropical Atlantic biases and their relation to surface wind stress and terrestrial precipitation. *Clim Dyn* 38(5–6):985–1001
- Sanga-Ngoie K, Fukuyama K (1996) Interannual and long-term climate variability over the Zaire River Basin over the last 30 years. *J Geophys Res* 101(D16):21351–21360
- Sprintall J, Tomczak M (1992) Evidence of the barrier layer in the surface layer of the Tropics. *J Geophys Res Ocean* 97(C5):7305–7316
- Stockdale TN, Balmaseda MA, Vidard A (2006) Tropical Atlantic SST prediction with coupled ocean-atmosphere GCMs. *J Clim* 19:6047–6061
- Todd MC, Washington R (2004) Climate variability in central equatorial Africa: Influence from the Atlantic sector. *Geophys Res Lett* 31(L23202). doi:10.1029/2004GL020975
- Uppala SM, Kalleberg PW, Simmons AJ, Andrae U, da ERA-40 reanalysis Berchtold V da Costa, Fiorino M, Gibson, JK, Haseler J, Hernandez A, Kelly GA, Li X, Saarinen S, Sokka N, Allan RP, Andersson E, Arpe K, Balmaseda MA, Beljaars ACM, Bidlot J, Van de Berg L, Bormann J, Caires S, Chevalier F, Dethof A, Dragosavac M, Fischer M, Fuentes M, Hagemann S, Holm E, Hosking BJ, Isaksen L, Janssen PA, Jenne R, McNally PA, Mahfouf JF, Morcrette JJ, Rayner NA, Saunders RW, Simon P,

- Sterl A, Trenberth KE, Untch A, Vasiljevic D, Viterbo P, Woolen J (2007) The ERA-40 reanalysis. *Q J R Met Soc* 131(612):2961–3012
- Van den Dool HM, Peng PT, Johansson A, Chelliah M, Shabbar A, Saha S (2006) Seasonal-to-decadal predictability and prediction of North American climate: the Atlantic influence. *J Clim* 19(23):6005–6024
- Vangriesheim A, Pierre C, Aminot A, Metzl N, Baurand F, Caprais JC (2009) The influence of Congo River discharges in the surface and deep layers of the Gulf of Guinea. *Deep-Sea Res II* 56(23):2183–2196
- Vinayachandran PN, Nanjundiah RS (2009) Indian Ocean sea surface salinity variations in a coupled model. *Clim Dyn* 33:245–263
- Vinayachandran PN, Murty VSN, Babu VR (2002) Observations of barrier layer formation in the Bay of Bengal during summer monsoon. *J Geophys Res Ocean* 107 (C12). doi:[10.1029/2001JC000831](https://doi.org/10.1029/2001JC000831)
- Weldeab S, Lea DW, Schneider RR, Andersen N (2007) 155,000 Years of West African monsoon and ocean thermal evolution. *Science* 316(5829):1303–1307
- Xie SP, Carton JA (2004) Tropical Atlantic variability: patterns, mechanisms, and impacts. In: Wang C, Xie S-P, Carton JA (eds) *Ocean-atmosphere interaction and climate variability*. AGU Press, Washington
- Yu L, Jin X, Weller RA (2008) Multidecade global flux datasets from the objectively analyzed air-sea fluxes (OAFlux) project: latent and sensible heat fluxes, ocean evaporation, and related surface meteorological variables. Woods Hole Oceanographic Institution, OAFlux Project Technical Report. OA-2008-01, 64 pp. Woods Hole, Massachusetts
- Zebiak SE (1993) Air-sea interactions in the equatorial Atlantic region. *J Clim* 6:1567–1586